Chapter 6

Contemporary Earthquake Hazards along the Himalayan Arc: A Statistical Perspective through Natural Times

"*Statistical thinking will one day be as necessary a qualification for efficient citizenship as the ability to read and write*"

by H. G. Wells

This chapter focuses on the computation of earthquake potential score in dozens of populous cities along the Himalayan arc through the concept of natural time analysis. Therefore, a combination of geodetically observed spatial distribution of earthquake potential (Chapter 3 to Chapter 5) may be complemented and corroborated with the statistically computed earthquake potential scores to highlight the regions of high seismic hazard.

Contents

Parts of this chapter have been submitted/published in the following refereed publications:

1. S. Pasari and **Y. Sharma**, "Contemporary earthquake hazards in the west-northwest Himalaya: a statistical perspective through natural times," *Seismological Research Letters*, vol. 91, pp. 3358–3369, 2020. (SCI)
(https://doi.org/10.1785/0220200104)

2. S. Pasari, **Y. Sharma**, and Neha "Quantifying the current state of earthquake hazards in Nepal," *Applied Computing and Geosciences*, vol. 10, p. 100058, 2021.
(https://doi.org/10.1016/j.acags.2021.100058)

3. S. Pasari, **Y. Sharma**, and Neha, "Spatial distribution of earthquake hazards in northeast India and Bangladesh regions inferred from natural time analysis." *Journal of Asian Earth Sciences: X* (Under review).

6.1 Introduction

The fear of seismic disaster has prevailed along the arcuate Himalayan belt and its adjoining areas, as the population in these regions started growing rapidly [30, 202, 225]. Geodynamical processes in the region suggest that the formation of Himalaya, picturesque intermontane valleys, duns, synclines, and anticlines result from the ongoing India-Eurasia continental-continental plate collision since 55 Ma [229, 257, 291]. Along with the Himalayan thrust system, several large-scale transverse faults and folds that are oblique or normal to the Himalayan tectonic trend have developed as a consequence of this collisional process [291, 320]. The entire portion of the Himalayan orogen observes a very high seismicity exhibiting a number of deadly earthquakes, such as the 1897 M_w=8.0 Shillong, 1905 M_w=7.8 Kangra, 1934 M_w=8.1 Bihar-Nepal, 1950 M_w=8.6 Assam, 1991 M_w=6.8 Uttarkashi, 1999 M_w=6.8 Chamoli, 2005 M_w=7.6 Kashmir, and the 2015 M_w=7.8 Nepal earthquake [8, 18, 30, 129]. These large size earthquakes not only retard the economic growth and successive development of the regions but also cause great destruction to the socio-economic infrastructure in the fertile Indo-Gangetic plain including several mega-cities [34, 29]. In this regard, using a dense GPS dataset, the previous chapters (Chapter 3 to Chapter 5) have determined strain accumulation, slip rates of the megathrust system, and spatial distribution of earthquake potential along the Himalayan arc, whereas the present chapter employs an "areal-source" based nowcasting analysis [246] of interevent earthquake counts in the Himalayan subcontinent to statistically determine the current level of seismic progression at dozens of populous cities in a rapid, consistent, and semi-automatic manner. The nowcasting method produces "earthquake potential score (EPS)", a numerical value (between 0 and 1) that can serve as a yardstick to determine the current level of earthquake hazard in a defined region.

Space-time correlation of fault networks and earthquake clustering [e.g., 256, 286], empirical scaling relationship, as illustrated by the Gutenberg-Richter frequency-magnitude power law and Omori's law of aftershock decay [e.g., 41, 265], spatio-temporal migration and switching mechanism of fault systems [e.g., 97, 256], streak and hierarchical fault plane geometry [e.g., 200, 203], macroscopic behavior (e.g., ergodicity and Boltzmann distributions in energy) of far-from-equilibrium earthquake dynamics [e.g., 71, 242, 243], and the time-series of an ordered pair of earthquake events (e.g., large and small) in a driven, nonlinear, self-organizing, strongly dissipative threshold system [e.g., 246, 294, 295] exhibit a wealth of information related to the study of earthquakes and consequent

hazard analysis. Although high-resolution geodetic measurements of crustal deformation provide precise information to the tectonic stress regime and earthquake fault kinematics in a defined area (as explained in Chapter 4 and Chapter 5), their observational timescales are certainly inadequate to characterize a complete seismic-cycle behavior [168]. Even in seismological observations, due to the shorter time-span of earthquake catalog, the concept of "seismic-cycle" that traditionally refers to the large repeating earthquakes in a specific fault segment, is slowly being revised to account for the recurrent events in a larger fault system comprising a variety of geological faults [79, 108, 211, 246]. Likewise, driven by the physical plausibility, the assumption of Poissonian distributed seismicity and associated time-independent seismic hazard evaluations [e.g., 80] have been relaxed in several recent implementations of the time-dependent seismic hazard estimations, including clustering based hazard assessment [e.g., 286], aftershock probabilistic seismic hazard estimation [e.g., 311], sequence-based probabilistic seismic hazard analysis [e.g., 79, 108], and many others [41, 256]. As a consequence, there has been a considerable amount of interest to develop innovative ways to empirically assess earthquake hazard for a strategic disaster mitigation planning. One of the major questions that have certainly garnered attention to the public, policymakers, and earthquake professionals is "what is the spatial distribution of current earthquake hazard and how far along is a city in the earthquake cycle of large sized events?"

In the present chapter, the concept of Natural Time Analysis (NTA) is employed to statistically address the problem related to the evaluation of the current state of seismic hazard at different cities along the Himalayan arc as well as its adjacent regions. The basic idea of NTA comes from the classical frequency-size power-law distribution of events driven by a complex process [294, 295]. Natural times, in seismology, refers to the counts of intermittent small magnitude events between pairs of large earthquakes in a defined area [246, 295]. Natural time counts essentially constitute a time domain that offers several notable properties in comparison to the calendar or clock time analysis. For example, upon considering an excerpt of a complete earthquake catalog comprising K cycles of large earthquake events, the NTA exhibits spatial (background seismicity rate) and clustering (seismicity declustering) invariability as long as the Gutenberg-Richter b-value remains unchanged in the entire region during the time span of the earthquake catalog [246, 294, 295]. As a consequence, the frequency-magnitude statistics in a spatially larger region presumably remains indifferent to the frequency-magnitude distribution in a smaller area, such as a circular city region. The ensemble NTA is uniformly valid to

any seismic region irrespective of whether it is predominantly controlled or partially influenced by aftershocks, background seismicity, induced seismicity, triggered earthquake sequences, or any such arising combination [156, 157, 246, 295]. Moreover, the inferential natural time statistics, when applied to a sub-excerpt of the catalog pertaining to a specified city region, allows scientists to statistically figure out EPS of the city [246]. With several such EPS values, the proposed framework enables ranking of a number of cities based on their present tectonic stress build-up since the last major event [213, 240, 244, 246].

The NTA, coupled with the related "nowcasting" technique, has found several exciting applications in seismic hazard assessment [156, 157, 213, 240, 244, 245, 246]. The method was applied to a dozens of global megacities including Ankara, Chile, Dhaka, Jakarta, Kolkata, Lima, Los Angeles, Manila, New Delhi, San Francisco, Taipei, and Tokyo to estimate their current state of seismic hazard [213, 216, 240, 246]. To examine the temporal progression of induced seismicity, the NTA was performed at the Groningen gas field in the Netherlands [e.g., 156], Geysers geothermal region, and the fluid injected sites in Oklahoma [e.g., 156]. Two of the recent applications of NTA have focused on the evidence of temporal clustering in global seismicity [e.g., 156] and the contemporary hazard analysis from great global earthquakes or mega-tsunamis [240, 245]. Efforts are also made to establish a possible connection of NTA to the statistical mechanics of earthquake kinematics explained through the ergodicity, information theory, percolation process, or phase transition [102, 241, 244, 246, 247, 294, 295].

In this chapter, the EPS scores at a dozen populous cities along the Himalayan subcontinent are calculated in order to statistically address the current state of regional earthquake hazard.

6.2 Study area and dataset

To calculate the current state of earthquake hazard along the Himalayan arc, the whole arc is divided into three broader segments, namely the northwest Himalaya, central Himalaya, and the northeast Himalaya. Further, the earthquake potential score is computed for all major cities that belong to these segments.

6.2.1 Northwest Himalaya

Lying in the sub-tropical zone with a semi-arid to arid climatic condition, the study region (68°– 83° E, 25°– 37° N) encompasses the northwest Himalaya and its surrounding regions of north-central India, east-northeast Pakistan and Hindu Kush mountain range (Fig. 6.1).

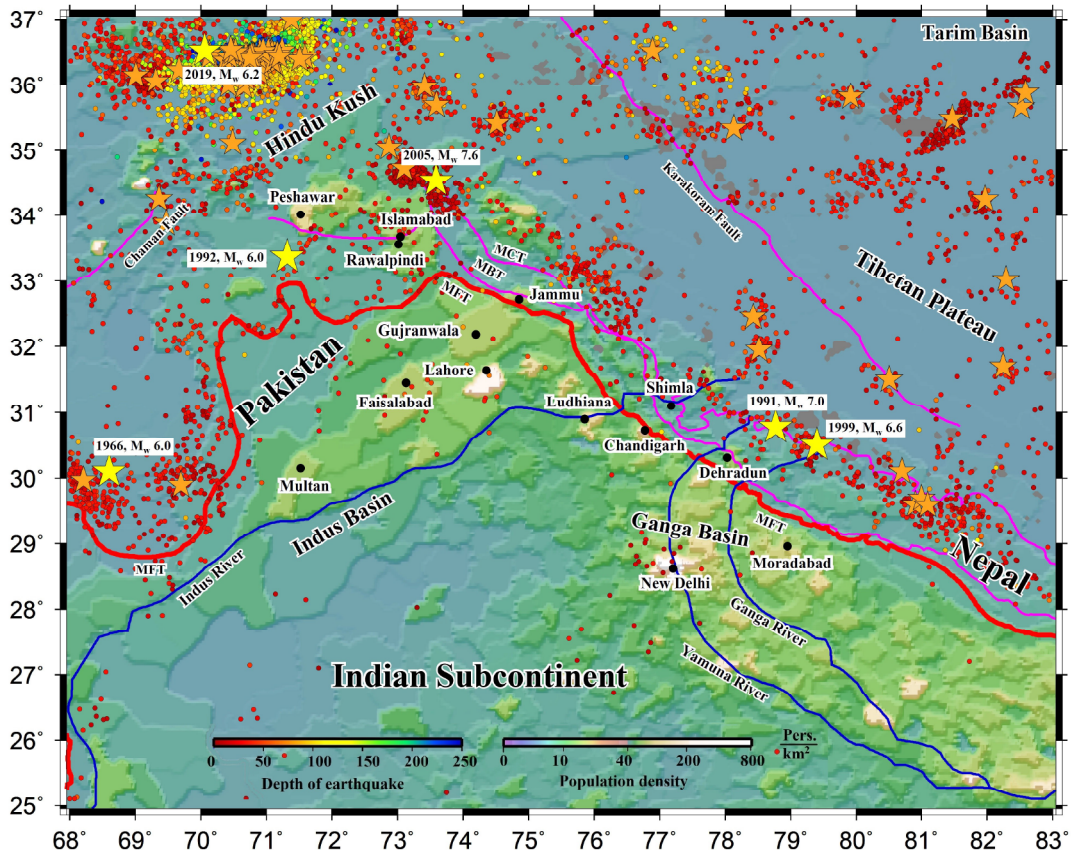

Fig. 6.1: Seismotectonic map of the northwest Himalaya and adjoining regions. The large magnitude earthquakes are represented by stars while the small earthquake events are represented by small circles. The background color of the figure represents the population density distribution in the study region [56].

The region bounded by the Tibetan Plateau in the east, Tarim block in northeast, Pamir Plateau in north, Tajik depression in northwest, Turan plate in west, Afghan block in southwest, Indian stable continental region in south, and the Lhasa block in the southeast exhibits an extremely complex seismotectonic structure [321]. The study region, comprising several duns, valleys, and fertile landforms, provides residence to ∼300 million

people from India, Pakistan, and surrounding countries (Fig. 6.1). The spatial distribution of current earthquake hazard in 14 major cities from India (New Delhi, Chandigarh, Dehradun, Jammu, Ludhiana, Moradabad, and Shimla) and Pakistan (Islamabad, Faisalabad, Gujranwala, Lahore, Multan, Peshawar, and Rawalpindi) is determined (Fig. 6.1). Since 1963, the study region along the northwest Himalaya has observed 7,942 events of M≥4, including 86 "large" events with M≥6.

6.2.2 Central Himalaya

In order to derive natural time statistics in the central Himalaya, the instrumental seismicity of Nepal and surrounding regions are considered.

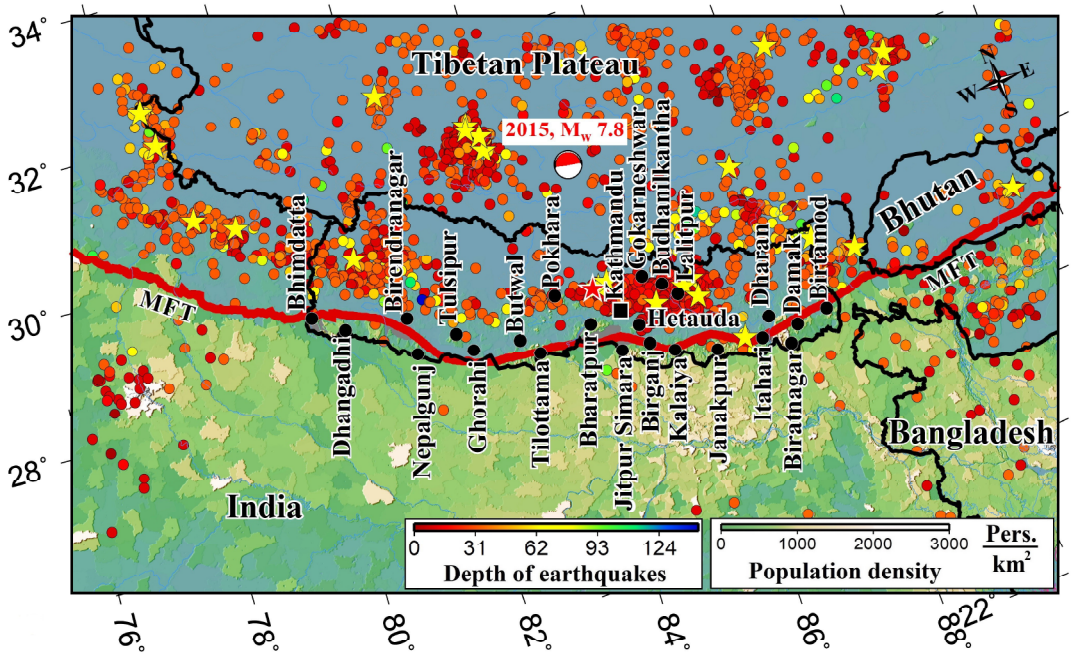

Fig. 6.2: Seismotectonic map of Nepal and surrounding regions. The background color indicates the population density of the area [56]. The thick red line shows the MFT. Earthquakes with magnitude M≥6.0 are represented by yellow stars. The black circles indicate the geographic center of 24 major cities. The colored circles represent seismicity (M≥4.0) in the study region.

The study region along the central Himalaya includes some part of the most-fertile IGP in the south and the Himalayan thrust belt in the north comprising four tectonostratigraphic zones: Tethys Himalaya, Greater Himalaya, Lower Himalaya, and Sub-Himalaya [179]. The study region comprising valleys, duns, and fertile river basins host several

large cities of Nepal with a total population of about ∼30 million people (Fig. 6.2). The spatial distribution of current earthquake hazard in 24 major cities of Nepal is determined. These cities are Kathmandu, Pokhara, Lalitpur, Bharatpur, Biratnagar, Birganj, Janakpur, Ghorahi, Hetauda, Dhangadhi, Tulsipur, Itahari, Nepalgunj, Butwal, Dharan, Kalaiya, Jitpur Simara, Birtamod, Damak, Budhanilkantha, Gokarneshwar, Bhimdatta, Birendranagar, and Tilotamma (Fig. 6.2). Since 1970, the study area along the central Nepal has observed 1764 events of M≥4, including 24 "large" earthquakes of M≥6.

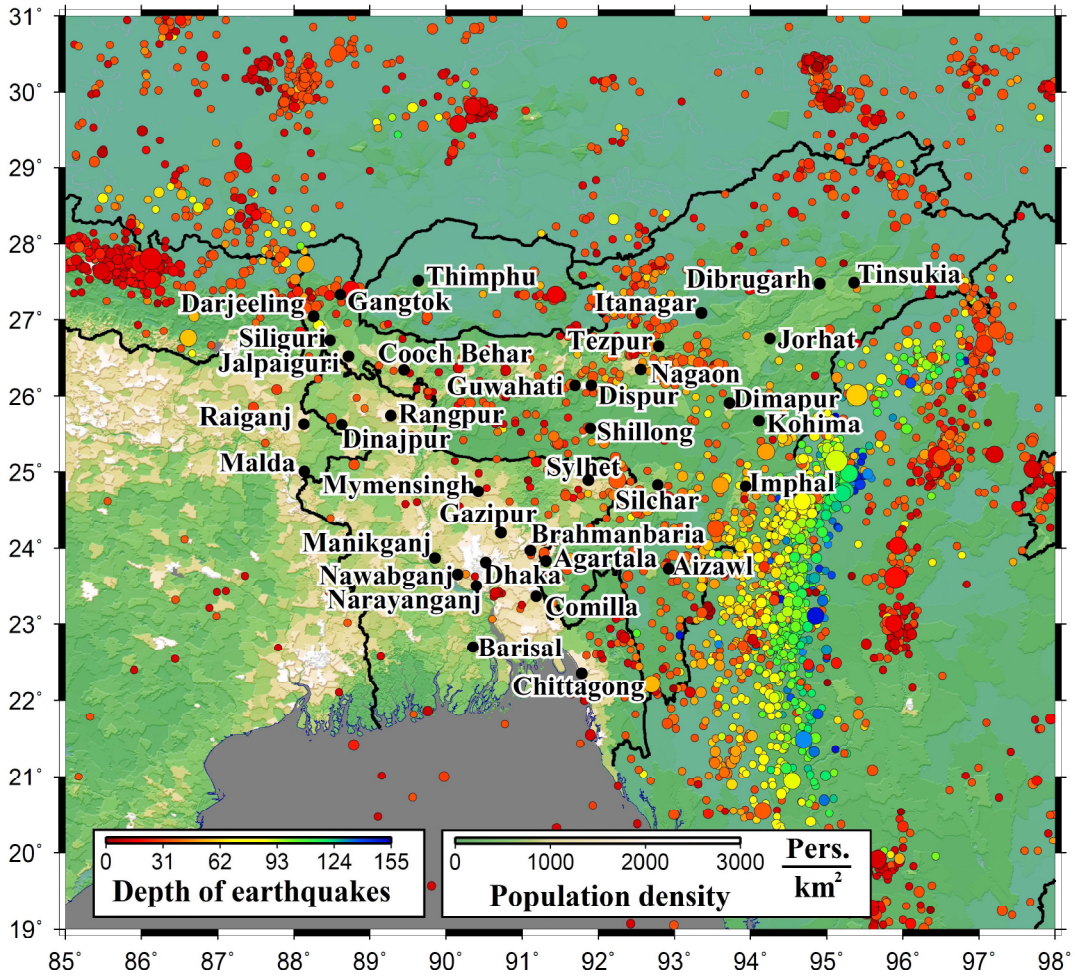

Fig. 6.3: Population density map of northeast Himalaya, Bengal Basin, Indo-Burma ranges, and adjoining regions [56]. The background color indicates population density in the study region. The black circle indicates the center of 36 cities. All earthquakes (M≥4) in the study region are represented by the colored circle, while the color of circles indicates depth and the size of circles represents the magnitude of earthquakes.

6.2.3 Northeast Himalaya

The study area in the northeast Himalaya is bounded by 19°N–31°N and 85°E–98°E. It comprises eastern part of Nepal, Bhutan, Bangladesh, part of China, hilly tracks of western Myanmar, and northeast India – a term that represents eight contiguous states of Arunachal Pradesh, Assam, Manipur, Meghalaya, Mizoram, Nagaland, Sikkim, and Tripura from northeast part of India. Part of West Bengal is also included in the study region. Due to the multi-plate interaction resulting in high seismicity, the northeast India region mostly falls under seismic zone V (severe risk zone) on the seismic zonation map of India. The study region comprising valleys, plain lands, and fertile river basins host several large cities with a total population of about 250 million people from India, Bangladesh, and neighboring countries (Fig. 6.3). These cities are: 22 cities from northeast India (Agartala, Aizawl, Dispur, Gangtok, Imphal, Itanagar, Kohima, Shillong, Darjeeling, Cooch Behar, Dibrugarh, Dimapur, Guwahati, Jalpaiguri, Jorhat, Malda, Nagaon, Raiganj, Silchar, Siliguri, Tezpur, and Tinsukia), the capital city of Bhutan (Thimphu), and 13 cities of Bangladesh (Barisal, Brahmanbaria, Chittagong, Comilla, Dhaka, Dinajpur, Gazipur, Manikganj, Mymensingh, Narayanganj, Nawabganj, Rangpur, and Sylhet). Since 1970, the study region along the northeast Himalaya has observed 3,562 events of M$\geq$4, including 40 "large" events with M$\geq$6.

6.3 Formulation of earthquake nowcasting method

Occurrence of earthquakes are random, though they are inferred to be quasi-periodic in seismic cycles [136, 256]. The irregularity in seismic "cycles" in a large geographic area has resulted into the formulation of different statistical measures based on a space-time organization of events [241, 246, 256]. The proposed method considers the ensemble statistics of recurring "natural times", intermittent small earthquake counts, to estimate the current level of seismic progression in terms of earthquake potential score (EPS). This empirical method is known as earthquake nowcasting [246].

To illustrate the nowcasting idea, let us consider a geographic region of area A and two magnitude thresholds (small and large) M_α and M_β. Let N_α and N_β denote the average cumulative count of earthquakes having magnitudes greater than M_α and M_β , respectively. Using Gutenberg-Richter scaling relation, the cumulative event count turns out to be $N_\alpha = 10^{a-bM_\alpha}$ and $N_\beta = 10^{a-bM_\beta}$ respectively, for some constants a and b.

Thus, the average number (N) of interevent small earthquakes (natural times) in a seismic cycle turns out to be

$$N = \frac{N_\alpha - N_\beta}{N_\beta} = 10^{\,b(M_\beta - M_\alpha)} \tag{6.1}$$

The above formulation shows that: (1) the NTA is independent to the productivity (a) of a spatial region, be it dominated by aftershocks or triggering events; (2) natural time count scales exponentially with the difference of the threshold magnitudes; and (3) particularly, with the assumption that b-value remains constant in time and space, the natural time (N) scales exponentially to the magnitude of large earthquakes, as the small magnitude threshold M_α, often deduced from the magnitude of completeness in a catalog (Fig. 6.4, Fig. 6.5, and Fig. 6.6), remains unchanged [246, 256]. As a consequence, unlike conventional hazard assessment methods, in nowcasting analysis, (1) dependent events have an equal opportunity to contribute to the analysis and (2) the fault "segmentation" concept can be dropped to account for a combined space-time interactions among a miscellany of faults and their associated "seismic cycles" [213, 240, 246].

To develop ensemble seismicity statistics for a given region A based on observed natural times (say, $N_1, N_2, ..., N_C$) corresponding to C number of earthquakes cycles, a group of reference probability distributions is employed to select the right data-derived cumulative distribution function (CDF). Assuming that natural time statistics remains invariant in space and time, the EPS for several local regions (say, $A_i, i = 1, 2, ..., k; A_i \subseteq A$) can be computed as $EPS_i \equiv F_N(m_i(t)) = P\{N \leq m_i(t)\}$, where $F_N(.)$ is the distribution of natural times and $m_i(t)$ is the current count of small events in the region A_i at clock (calendar) time t [246]. It may be noted that ergodic principle in the statistical mechanics of earthquake physics provides a theoretical ground for the above assumption in nowcasting analysis [241, 246].

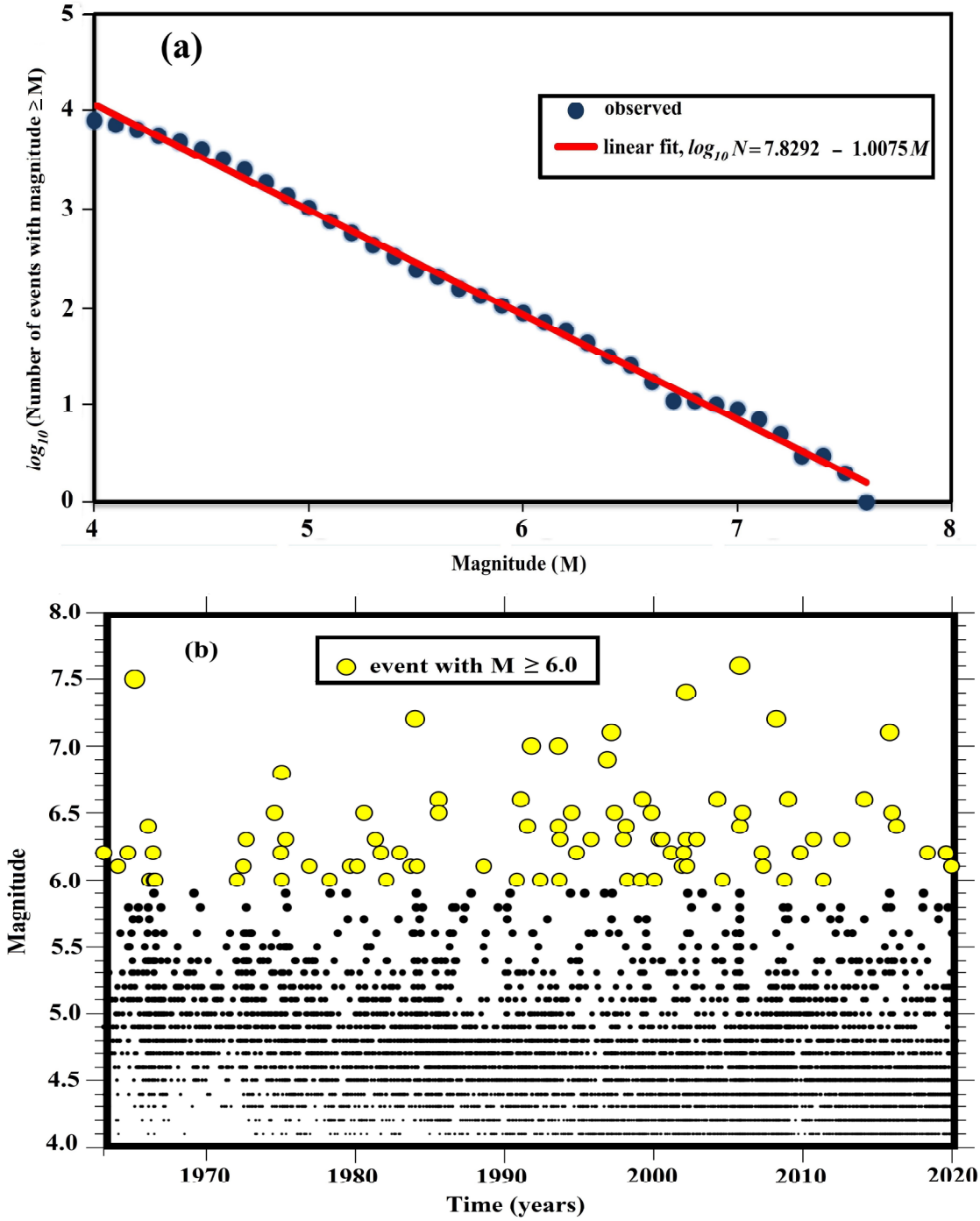

Fig. 6.4: (a) Frequency-magnitude plot and (b) magnitude-time graph for the present earthquake catalog in the northwest Himalaya.

Besides, it may be emphasized that earthquake nowcasting conceptually differs from earthquake forecasting in which the probability of a future event is estimated [246].

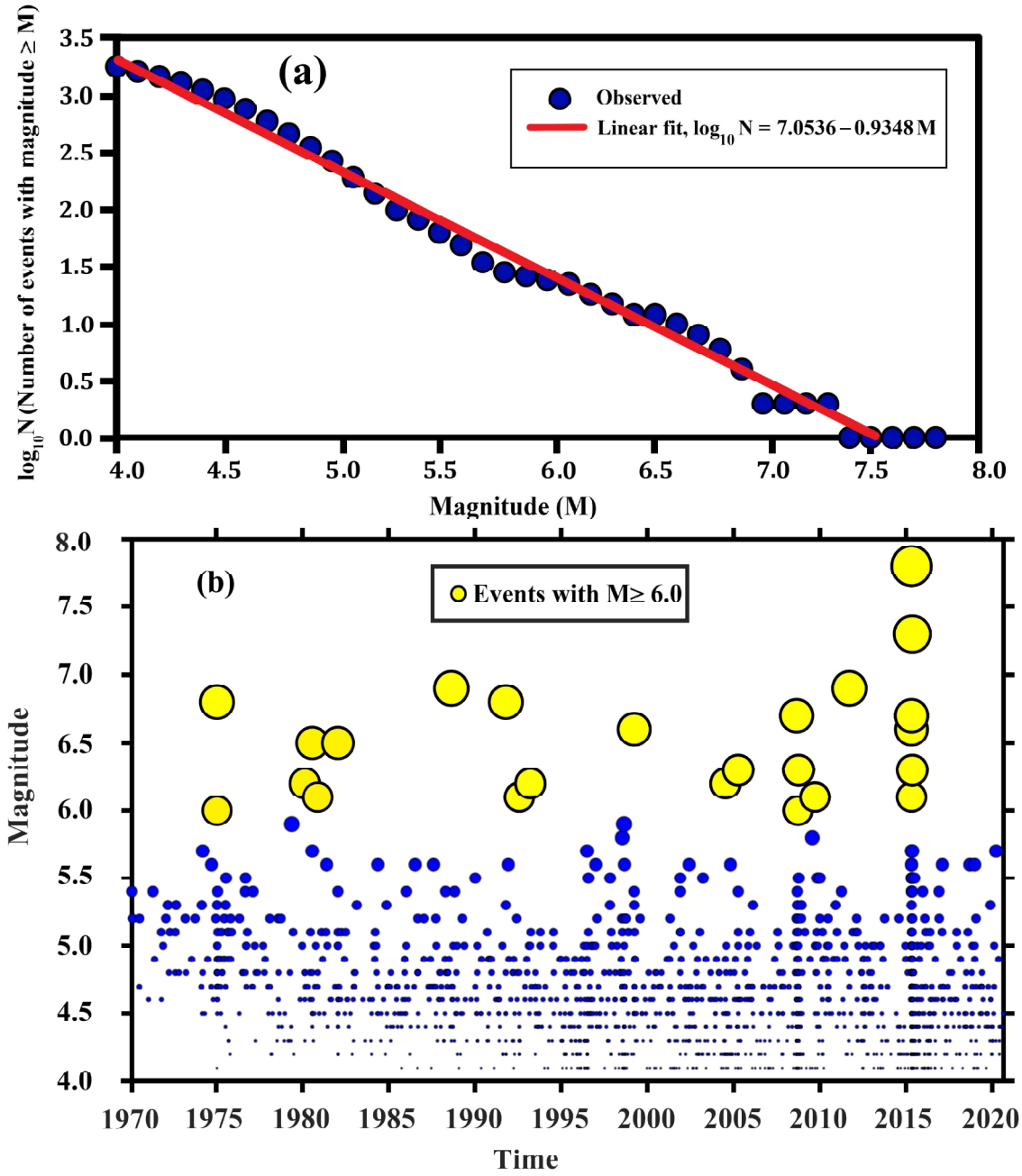

Fig. 6.5: (a) Frequency-magnitude plot and (b) magnitude-time graph for the present earthquake catalog in the central Himalaya.

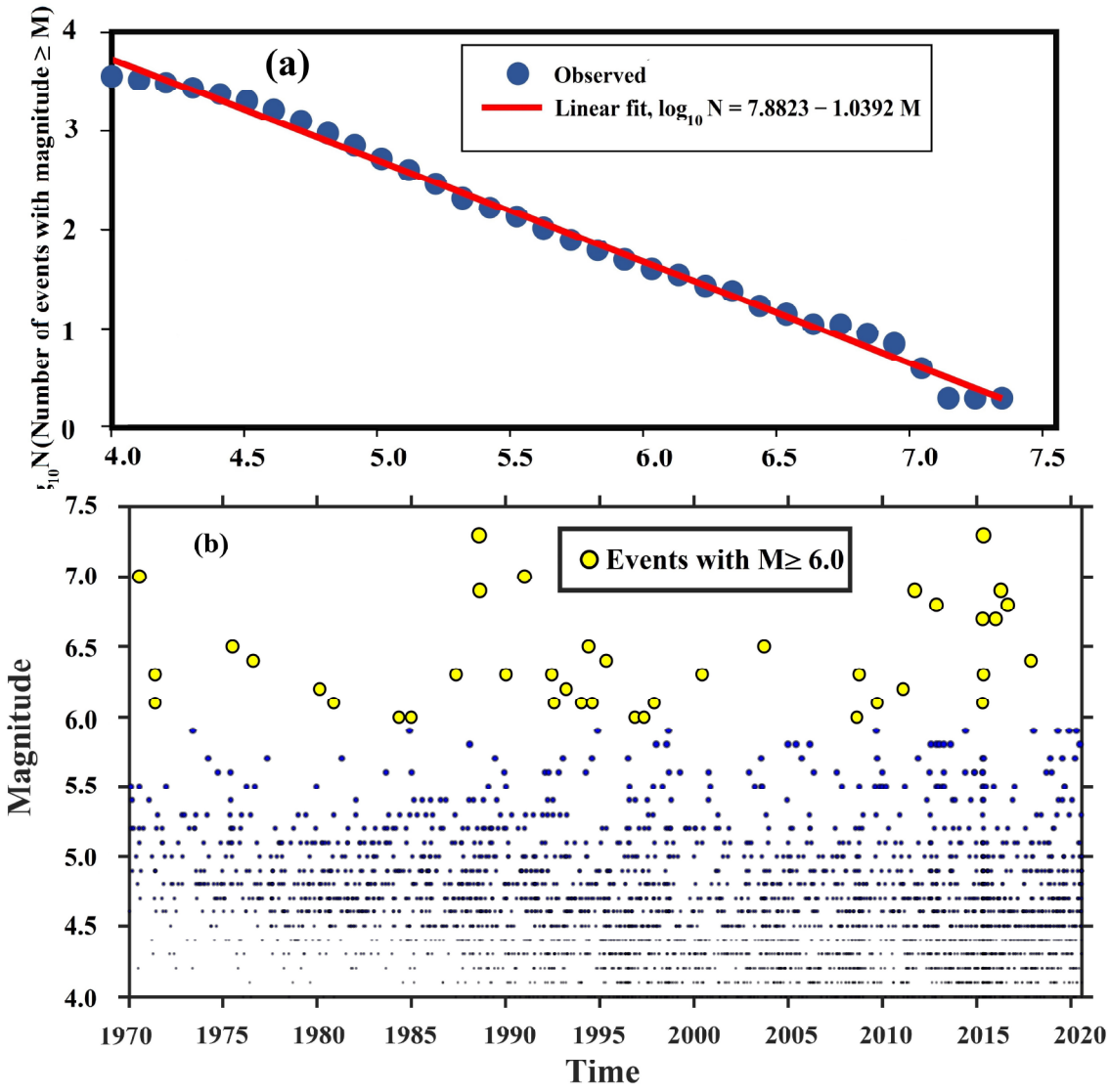

Fig. 6.6: (a) Frequency-magnitude plot and (b) magnitude-time graph for the present earthquake catalog in the northeast Himalaya.

The methodology adopted in a nowcasting analysis consists of three broad steps: preparing data (natural times) for the study region, deriving seismicity statistics of natural times, and computing earthquake potential score (nowcast scores) for a number of cities embedded in the study region. A simple flowchart of the earthquake nowcasting approach is illustrated in Fig. 6.7. While the description of "small" (say, $M4$) and "large" (say, $M6$) events in data preparation (Step-1) usually comes from the notion of magnitude completeness threshold (Fig. 6.4, Fig. 6.5, and Fig. 6.6) and societal destruction, deriving natural time statistics (Step-2) requires probability model description, parameter estimation, and model selection. Using the best-fit cumulative distribution of natural

times in the entire study region (in Step-2), the nowcast values for several circular city regions are computed to measure their current state of earthquake hazards.

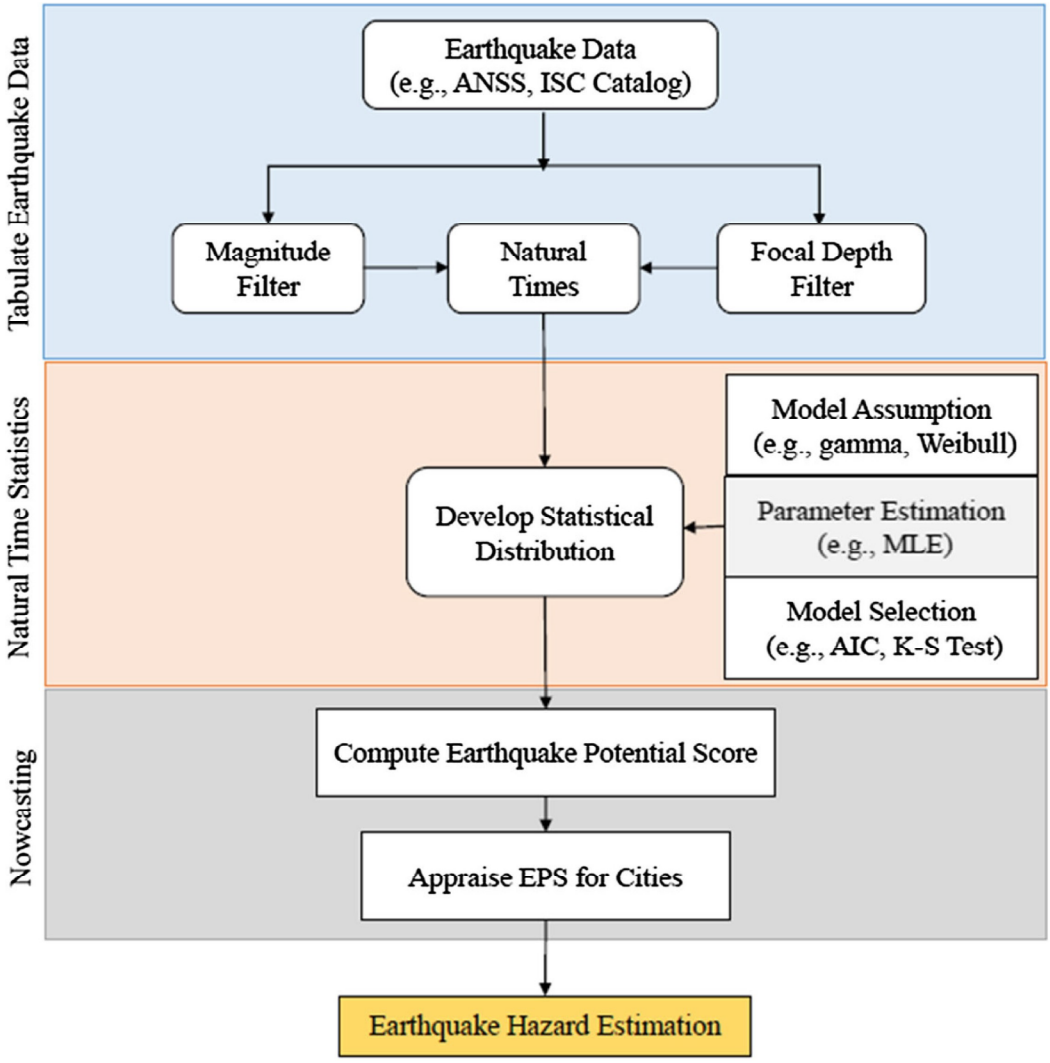

Fig. 6.7: Flowchart of the nowcasting approach for earthquake hazard estimation [213].

Table 6.1: Probability distribution models

Distribution	Density function (t>0)	Parameter domain
Exponential	$\frac{1}{\alpha} exp\left[-\frac{t}{\alpha}\right]$	$\alpha > 0$
Gamma	$\frac{1}{\Gamma(\beta)} \frac{t\beta-1}{\alpha^{\beta}} exp\left[-\frac{t}{\alpha}\right]$	$\alpha, \beta > 0$

Weibull	$\frac{\beta}{\alpha}t^{\beta-1}exp\left[-\left(\frac{t}{\alpha}\right)^{\beta}\right]$	$\alpha,\beta>0$
Exponentiated Exponential	$\alpha\beta\left(1-exp\left[-\alpha t\right]\right)^{\beta-1}exp\left[-\alpha t\right]$	$\alpha,\beta>0$
Exponentiated Weibull	$\frac{\beta\gamma}{\alpha}\left(\frac{t}{\alpha}\right)^{\beta-1}exp\left[\left(\frac{t}{\alpha}\right)^{\beta}\right]\left(1-exp\left[\left(\frac{t}{\alpha}\right)^{\beta}\right]\right)^{\gamma-1}$	$\alpha,\beta,\gamma>0$

Table 6.2: Parameter estimation of selected probability distribution and model selection results corresponding to the observed natural times of the study region

Region	Distribution	Statistical Inference	
		MLE	K-S
Northwest Himalaya	Exponential	$\hat{\alpha}$=94.9634	0.0727
	Gamma	$\hat{\alpha}$=111.0609, $\hat{\beta}$=0.8551	0.0790
	Weibull (Best-fit)	$\hat{\alpha}$=94.2239, $\hat{\beta}$=0.9825	0.0663
	Exponentiated Exponential	$\hat{\alpha}$=95.5773, $\hat{\beta}$=0.9901	0.0708
	Exponentiated Weibull	$\hat{\alpha}$=65.7269, $\hat{\beta}$=0.8244, $\hat{\gamma}$=1.4682	0.0715
Central Himalaya	Exponential (Best-fit)	$\hat{\alpha}$=65.0470	0.1406
	Gamma	$\hat{\alpha}$=60.9987, $\hat{\beta}$=1.0663	0.1534
	Weibull	$\hat{\alpha}$=65.8903, $\hat{\beta}$=1.0313	0.1501
	Exponentiated Exponential	$\hat{\alpha}$=62.2928, $\hat{\beta}$=1.0700	0.1533
	Exponentiated Weibull	$\hat{\alpha}$=42.7487, $\hat{\beta}$=0.8053, $\hat{\gamma}$=1.5614	0.1525
Northeast Himalaya	Exponential	$\hat{\alpha}$=82.1282	0.1141
	Gamma	$\hat{\alpha}$=88.3351, $\hat{\beta}$=0.9513	0.1228
	Weibull (Best-fit)	$\hat{\alpha}$=83.7543, $\hat{\beta}$=1.0501	0.0982
	Exponentiated Exponential	$\hat{\alpha}$=77.5338, $\hat{\beta}$=1.0945	0.0997

Exponentiated Weibull	$\hat{\alpha}$=73.7174, $\hat{\beta}$=0.7660, $\hat{\gamma}$=2.0077	0.1008

To perform NTA on the dataset, a parametric family of five probability distributions is employed having positive real line as their domain. As the actual magnitude of large earthquake varies from event to event, the natural time count varies for each earthquake cycle. Thus, it is reasonable to consider exponential distribution and its primary variants gamma, Weibull, and exponentiated exponential in developing the data-derived cumulative distribution function (CDF) and associated earthquake potential score (EPS) computation (Table 6.1). Using the maximum likelihood method and the non-parametric Kolmogorov-Smirnov (K-S) statistic, model parameters are estimated and the best-fit distribution is determined for the observed event counts [211]. While the maximum likelihood technique involves maximizing the likelihood function of the unknown population parameters for a given set of observations, the non-parametric K-S procedure ranks candidate probability models based on their (minimum) vertical distances between the two distribution functions: empirical data distribution and the reference cumulative distribution. It may be noted that the non-parametric K-S test provides a robust model validation technique in a way that it is not only free from any specific a-priori distributional assumption (e.g., Gaussian), but also performs well under a wide range of reference population distributions. It is found that the Weibull distribution provides the best representation to the observed natural times for the northwest and the northeast Himalaya, whereas the exponential distribution is deemed to be the best-fit model for the present dataset in the central Himalaya (Table 6.2).

6.4 Results

Considering the small event magnitude threshold M_α=4.0, large event magnitude threshold M_β=6.0, and the radius of circular city region R=300 km for the northwest, and R=250 km for both of the central and the northeast Himalaya, the nowcast score of 74 cities from India, Pakistan, Nepal, Bhutan, and Bangladesh is calculated.

6.4.1 EPS at several cities along the northwest Himalaya

Results reveal that the Indian cities New Delhi, Chandigarh, Dehradun, Jammu, Ludhiana, Moradabad, and Shimla have EPS values of about 56, 86, 83, 99, 89, 84, and 87 percentage, respectively, whereas the cities Islamabad, Faisalabad, Gujranwala, Lahore, Multan, Peshawar, and Rawalpindi in Pakistan have their EPS scores 99, 88, 99, 89, 98, 38, and 99 percentage, respectively (Table 6.3 and Fig. 6.8). Physically, this result indicates, for example, that the capital city New Delhi has progressed about half of the way through its cycle of magnitude 6.0 or higher events, while the capital city Islamabad has reached the rear end of its earthquake cycle.

Table 6.3: Earthquake potential scores for $M \geq 6.0$ events in 14 major cities along the northwest Himalaya corresponding to M_α=4.0 and R=300 km

City	City center		Date of last large event	Magnitude of last large event	Current small event count	EPS (%)
	Lat (°N)	Long (°E)				
New Delhi	28.6139	77.2090	28/03/1999	6.6	78	56
Chandigarh	30.7333	76.7794	28/03/1999	6.6	188	86
Dehradun	30.3165	78.0322	28/03/1999	6.6	170	83
Jammu	32.7266	74.8570	08/10/2005	7.6	459	99
Ludhiana	30.9010	75.8573	19/10/1991	7.0	210	89
Moradabad	28.8386	78.7733	28/03/1999	6.6	175	84
Shimla	31.1048	77.1734	28/03/1999	6.6	193	87
Islamabad	33.6844	73.0479	08/10/2005	7.6	520	99
Faisalabad	31.4504	73.1350	20/05/1992	6.0	200	88
Gujranwala	32.1877	74.1945	08/10/2005	7.6	438	99
Lahore	31.6400	74.3587	08/10/2005	7.6	209	89
Multan	30.1575	71.5249	01/08/1966	6.0	357	98
Peshawar	34.0151	71.5249	20/12/2019	6.1	45	38

Rawalpindi	33.5651	73.0169	08/10/2005	7.6	490	99

6.4.2 EPS at several cities along the central Himalaya

It is observed that the present analysis assigns EPS values between 59% and 99% to 24 major cities of Nepal, with the scores (%) of six metropolitan areas Kathmandu (95), Pokhara (93), Lalitpur (95), Bharatpur (93), Biratnagar (92), and Birganj (93). Eleven sub-metropolitan cities have EPS (%) as Janakpur (95), Ghorahi (67), Hetauda (93), Dhangadhi (94), Tulsipur (59), Itahari (93), Nepalgunj (97), Butwal (96), Dharan (93), Kalaiya (93), and Jitpur Simara (93), whereas seven municipality areas with population higher than 100,000 (according to 2011 census) observe nowcast scores (%) as Birtamod (89), Damak (92), Budhanilkantha (95), Gokarneshwar (95), Bhimdatta (94), Birendranagar (99), and Tilotamma (97) (Table 6.4). However, it should be emphasized that the presently revealed stationary Poisson nature of the natural time statistics in Nepal Himalaya indicates that the risk is the same for all 24 circular city regions despite their different current levels of cycle progression realized through EPS values. Moreover, though the EPS values will be updated as each small earthquake occurs, the risk remains the same throughout the study region.

Table 6.4: Earthquake potential scores for $M \geq 6.0$ events in 24 major cities along the central Himalaya corresponding to M_α=4.0 and R=250 km

City	City center		Date of last large event	Magnitude of last large event	Current small event count	EPS (%)
	Lat (°N)	Long (°E)				
Bharatpur	27.6706	84.4385	12-05-2015	7.3	173	93
Bhimdatta	28.9873	80.1652	28-03-1999	6.6	187	94
Biratnagar	26.4525	87.2718	12-05-2015	7.3	166	92
Birendranagar	28.5776	81.6254	29-07-1980	6.5	282	99
Birganj	27.0449	84.8672	12-05-2015	7.3	169	93
Birtamod	26.6293	87.9825	12-05-2015	7.3	141	89

Budhanilkantha	27.7654	85.3653	12-05-2015	7.3	195	95
Butwal	27.6866	83.4323	25-04-2015	7.8	214	96
Damak	26.6717	87.6680	12-05-2015	7.3	161	92
Dhangadhi	28.6852	80.6216	28-03-1999	6.6	186	94
Dharan	26.8143	87.2797	12-05-2015	7.3	177	93
Ghorahi	28.0588	82.4861	25-04-2015	7.8	72	67
Gokarneshwar	27.7668	85.4066	12-05-2015	7.3	198	95
Hetauda	27.4368	85.0026	12-05-2015	7.3	175	93
Itahari	26.6646	87.2718	12-05-2015	7.3	174	93
Janakpur	26.7271	85.9407	12-05-2015	7.3	191	95
Jitpur Simara	27.1775	84.7237	12-05-2015	7.3	171	93
Kalaiya	27.0323	85.0078	12-05-2015	7.3	171	93
Kathmandu	27.7172	85.3240	12-05-2015	7.3	194	95
Lalitpur	27.6588	85.3247	12-05-2015	7.3	193	95
Nepalgunj	28.0548	81.6145	29-07-1980	6.5	233	97
Pokhara	28.2096	83.9856	12-05-2015	7.3	175	93
Tilottama	27.6193	83.4750	25-04-2015	7.8	221	97
Tulsipur	28.1309	82.2972	25-04-2015	7.8	58	59

6.4.3 EPS at several cities along the northeast Himalaya

The nowcast values for cities along the northeast Himalaya lie between 41% and 94%, with the EPS scores (%) of eight state capital cities from northeast India as Agartala (91), Aizawl (84), Dispur (42), Gangtok (65), Imphal (90), Itanagar (48), Kohima (85), and Shillong (52). Other cities from east-northeast part of India observe an EPS (%) as Darjeeling (81), Cooch Behar (58), Dibrugarh (49), Dimapur (80), Guwahati (41), Jalpaiguri (64), Jorhat (70), Malda (70), Nagaon (57), Raiganj (44), Silchar (87), Siliguri (73), Tezpur (51) and Tinsukia (47). The capital city of Bhutan, Thimphu, has a score

of 67 percent, whereas the 13 cities of Bangladesh observe an EPS (%) as Barisal (59), Brahmanbaria (90), Chittagong (94), Comilla (88), Dhaka (78), Dinajpur (48), Gazipur (79), Manikganj (70), Mymensingh (81), Narayanganj (77), Nawabganj (72), Rangpur (55) and Sylhet (60). These EPS scores provide an index on how far along is a city in the earthquake cycle of large sized events. At this juncture, it is important to note that the EPS scores for several large cities including Kolkata, Bogra, Rajshahi, Kushtia, Jessore, and Khulna are not determined, as these city regions have not experienced any large magnitude earthquake since 1970.

Table 6.5: Earthquake potential scores for $M \geq 6.0$ events in 14 major cities along the northeast Himalaya corresponding to M_α=4.0 and R=250 km

City	City center		Date of last large event	Magnitude of last large event	Current small event count	EPS (%)
	Lat (°N)	Long (°E)				
Agartala	23.8315	91.2868	21.11.1997	6.1	197	91
Aizawl	23.7307	92.7173	13.04.2016	6.9	151	84
Darjeeling	27.0410	88.2663	12.05.2015	6.3	136	81
Dibrugarh	27.4728	94.9120	17.11.2017	6.4	57	49
Dimapur	25.9091	93.7266	03.01.2016	6.7	130	80
Dispur	26.1433	91.7898	03.01.2016	6.7	47	42
Gangtok	27.3314	88.6138	12.05.2015	6.3	87	65
Guwahati	26.1445	91.7362	03.01.2016	6.7	45	41
Imphal	24.8170	93.9368	13.04.2016	6.9	185	90
Itanagar	27.0844	93.6053	03.01.2016	6.7	56	48
Jorhat	26.7509	94.2037	03.01.2016	6.7	99	70
Kohima	25.6751	94.1086	03.01.2016	6.7	153	85
Shillong	25.5788	91.8933	03.01.2016	6.7	63	52
Silchar	24.8333	92.7789	03.01.2016	6.7	163	87
Tezpur	26.6528	92.7926	03.01.2016	6.7	60	51

Tinsukia	27.4886	95.3558	17.11.2017	6.4	55	47
Nagaon	26.3480	92.6838	03.01.2016	6.7	71	57
Dhaka	23.8103	90.4125	08.05.1997	6.0	124	78
Comilla	23.4607	91.1809	21.11.1997	6.1	170	88
Sylhet	24.8949	91.8687	03.01.2016	6.7	77	60
Mymensingh	24.7471	90.4203	08.05.1997	6.0	134	81
Rangpur	25.7439	89.2752	18.09.2011	6.9	67	55
Narayanganj	23.6238	90.5000	08.05.1997	6.0	120	77
Manikganj	23.8644	90.0047	08.05.1997	6.0	99	70
Barisal	22.7010	90.3535	21.11.1997	6.1	76	59
Chittagong	22.3569	91.7832	21.11.1997	6.1	230	94
Nawabganj	23.6531	90.1518	08.05.1997	6.0	106	72
Brahmanbaria	23.9695	91.1119	21.11.1997	6.1	182	90
Dinajpur	25.6279	88.6332	18.09.2011	6.9	56	48
Gazipur	23.9999	90.4203	08.05.1997	6.0	129	79
Thimphu	27.5142	89.6339	18.09.2011	6.9	92	67
Raigang	25.6329	88.1319	18.09.2011	6.9	50	44
Siliguri	26.7271	88.3953	12.05.2015	6.3	109	73
Malda	25.0108	88.1411	20.08.1988	6.9	99	70
Jalpaiguri	26.5215	88.7196	18.09.2011	6.9	86	64
Cooch Behar	26.3452	89.4482	18.09.2011	6.9	74	58

The non-decreasing EPS scores, viewed as a way of tectonic stress accumulation since the last event [see, 245, 246], not only provide a realistic estimate on how far along is a city in its earthquake cycle of large sized events at current time, but also enables a systematic ranking of the cities based on their current exposure to earthquake risk. Overall, it is observed that the EPS scores for most of the cities along the Himalayan subcontinent

are observed to lie in the range of 80% and 99%. The high EPS scores indicate that these cities have reached to their rear end in the seismic cycle of large earthquakes.

6.5 Sensitivity analysis

To examine the overall consistency of the natural-time induced nowcast scores that are generated for a set of input parameters, a sensitivity testing on two parameters (i.e., small-magnitude threshold and circular city radius) is performed by (a) varying city radius R= 250, 300, 350 km (for the northwest Himalaya) and R=200, 250, 300 km (for the central and the northeast Himalaya) with fixed small magnitude threshold M_α=4.0 and (b) varying M_α=4.0, 4.5 with fixed city radius R= 300 km (for the northwest Himalaya) and R=250 km (for the central and the northeast Himalaya). In the sensitivity analysis, the case of M_α=3.5 is not considered as the catalog has a completeness threshold M_C=4 (Fig. 6.4, Fig. 6.5, and Fig. 6.6). Similarly, a sensitivity testing corresponding to M_β=6.5 is also not performed, because the number of seismic cycles significantly reduces to derive a reliable natural time statistics of the study region. The entire process of NTA is repeated for each of these different combinations and the EPS scores are pictorially represented in Fig. 6.8, Fig. 6.9, and Fig. 6.10.

The results suggest that the EPS values are generally consistent across all parameters except a few variations. As a generic observation, the EPS values steadily increase as the city radius increases, though, at times, the enlarged city radius may involve a recent large event lowering the EPS score (e.g., Peshawar with M_α=4.0 and R=250, 300 km; Rawalpindi with M_α=4.0 and R=250, 300 km; Agartala with M_α=4.0 and R=250, 300 km; Brahmanbaria with M_α=4.0 and R=250, 300 km; Comilla with M_α=4.0 and R=250, 300 km). Overall, Fig. 6.8, Fig. 6.9, and Fig. 6.10 show that EPS values are generally consistent to the changes of the input parameters, ensuring a consistent city ranking.

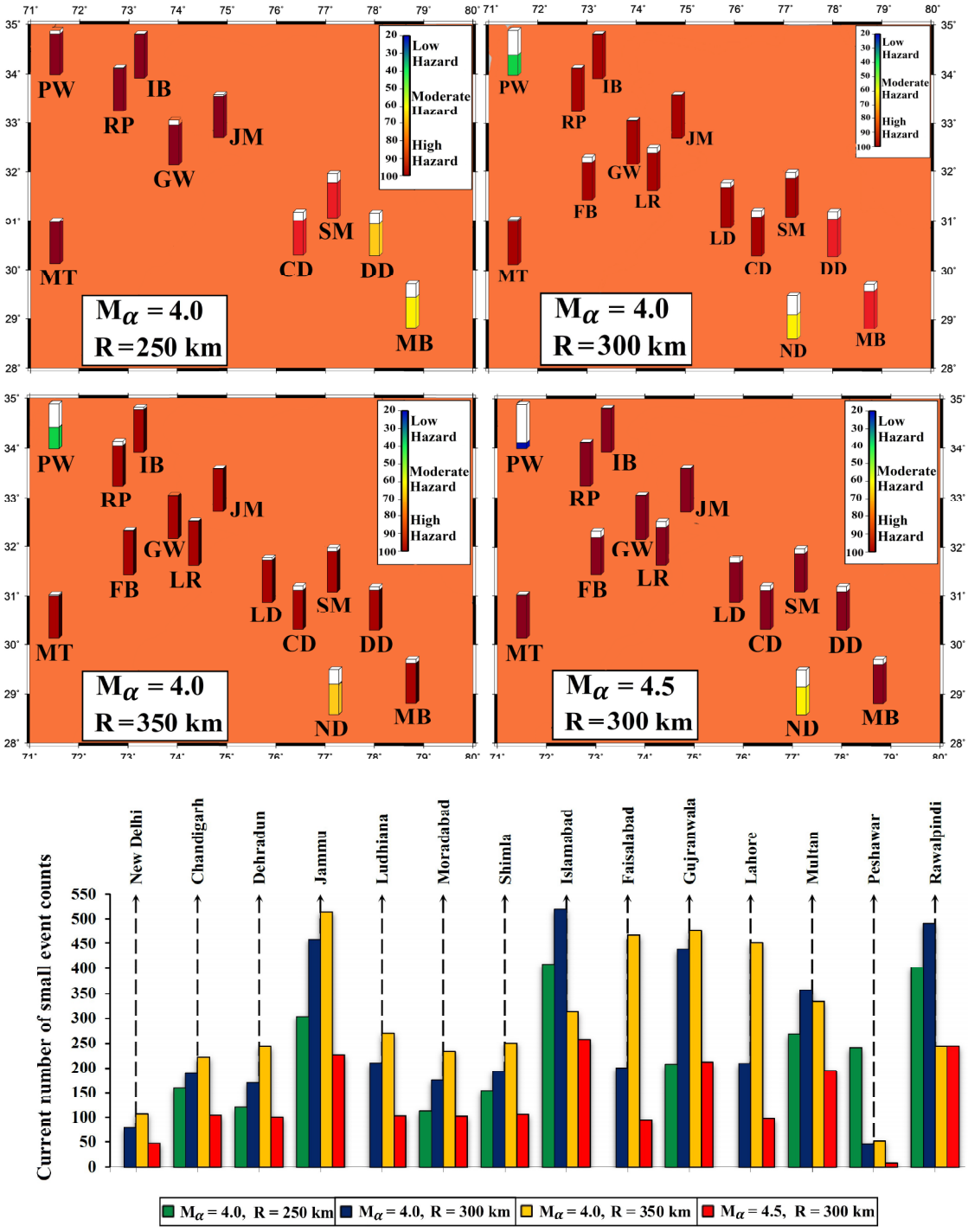

Fig. 6.8: The small magnitude threshold for the first three panels (a, b, c) is M_α=4.0 with varying city radius R=250, 300, 350 km whereas it is M_α=4.5 in the fourth panel (d) with radius R=300 km. The stacked bar-chart in the lower panel of the figure shows a comparison of the current number of small event counts at several city areas. Abbreviations for city names are as follows: CD, Chandigarh; DD, Dehradun; JM, Jammu; LD, Ludhiana; MB, Moradabad; ND, New Delhi; SM, Shimla; FB, Faisalabad; GW, Gujranwala; IB, Islamabad; LR, Lahore; MT, Multan; PW, Peshawar; RP, Rawalpindi.

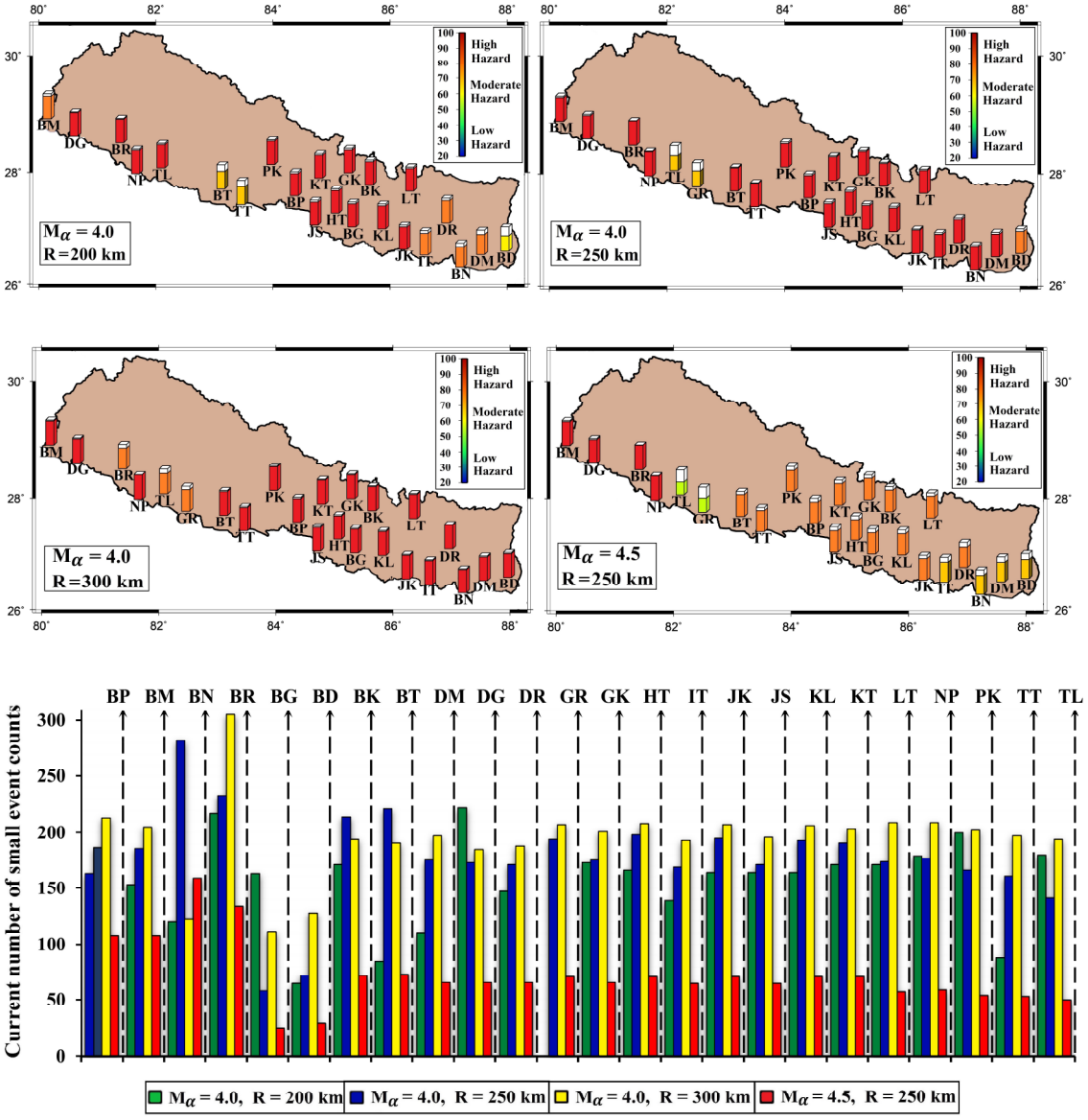

Fig. 6.9: The small magnitude threshold for the first three panels (a, b, c) is M_α=4.0 with varying city radius R=200, 250, 300 km whereas it is M_α=4.5 in the fourth panel (d) with radius R=250 km. The stacked bar-chart in the lower panel of the figure shows a comparison of the current number of small event counts at several city areas. Abbreviations for city names are as follows: BP, Bharatpur; BM, Bhimdatta; BN, Biratnagar; BR, Birendranagar; BG, Birganj; BD, Birtamod; BK, Budhanilkantha; BT, Butwal; DM, Damak; DG, Dhangadhi; DR, Dharan; GR, Ghorahi; GK, Gokarneshwar; HT, Hetauda; IT, Itahari; JK, Janakpur; JS, Jitpur Simara; KL, Kalaiya; KT, Kathmandu; LT, Lalitpur; NP, Nepalgunj; PK, Pokhara; TT, Tilottama; TL, Tulsipur. These EPS values, however, bear no information of the current level of earthquake hazards due to the Poisson nature of the underlying natural time statistics.

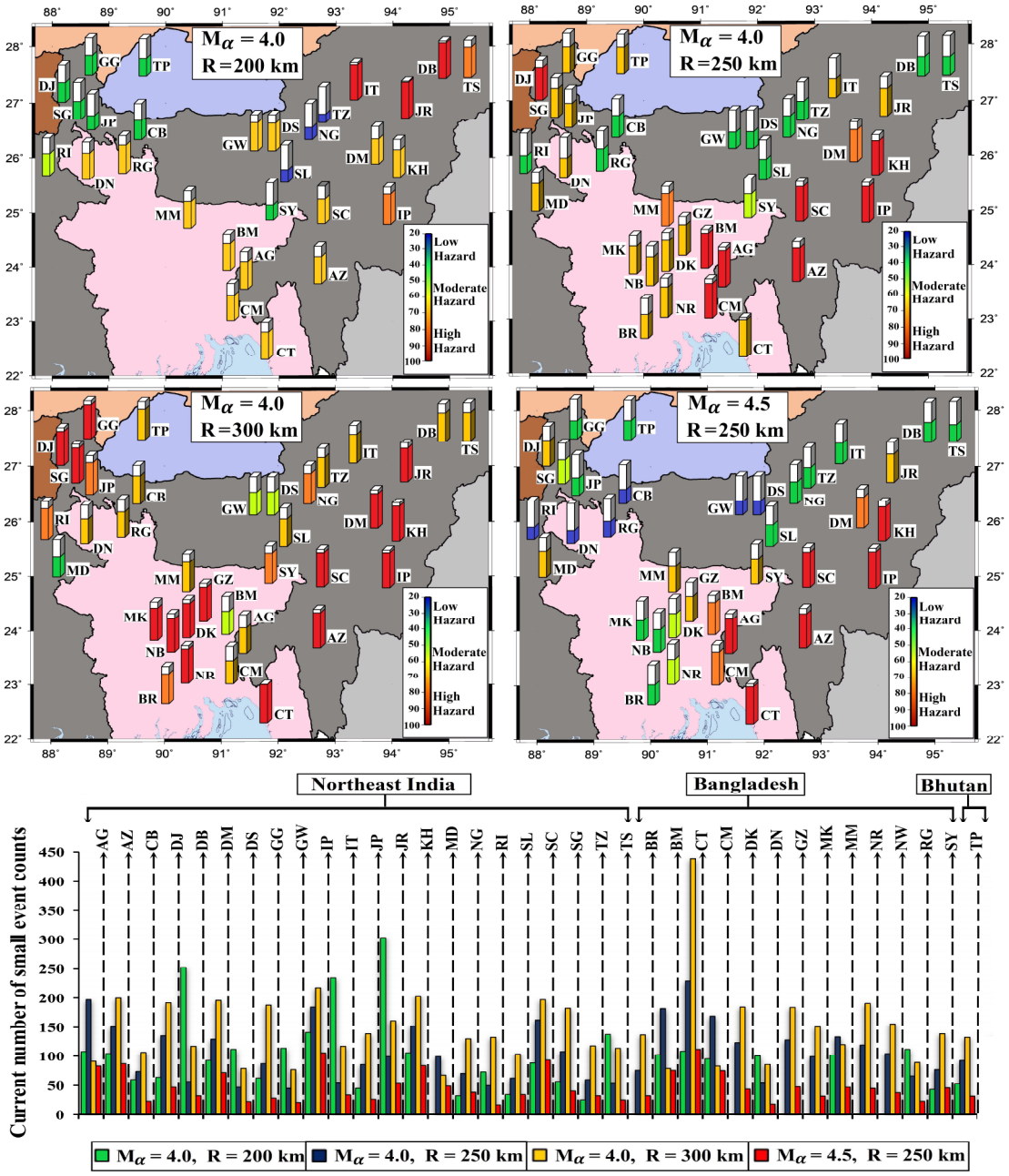

Fig. 6.10: The small magnitude threshold for the first three panels (a, b, c) is M_α=4.0 with varying city radius R=200, 250, 300 km whereas it is M_α=4.5 in the fourth panel (d) with radius R=250 km. The stacked bar-chart in the lower panel of the figure shows a comparison of the current number of small event counts at several city areas. Abbreviations are as follows: AG, Agartala; AZ, Aizawl; DS, Dispur; GG, Gangtok; IP, Imphal; IT, Itanagar; KH, Kohima; SL, Shillong; DJ, Darjeeling; CB, Cooch Behar; DB, Dibrugarh; DM, Dimapur; GW, Guwahati; JP, Jalpaiguri; JR, Jorhat; ML, Malda; NG, Nagaon; RI, Raiganj; SC, Silchar; SG, Siliguri; TZ, Tezpur; TS, Tinsukia; TP, Thimphu; BR, Barisal; BM, Brahmanbaria; CT, Chittagong; CM, Comilla; DK, Dhaka; DN, Dinajpur; GZ, Gazipur; MK, Manikganj; MM, Mymensingh; NR, Narayanganj; NB, Nawabganj; RG, Rangpur; SY, Sylhet.

6.6 Discussion

Seismicity is a driven complex process featuring space-time correlation in which earthquake occurrences are broadly aligned with a frequency-magnitude spectrum [256]. Statistical analysis of seismicity through natural times, cumulative small event counts between large earthquakes, allows us to characterize the current state of the regional fault system, without any distinction among mainshock, aftershock, or triggered events [246]. In the present study, a natural time analysis (NTA) is implemented in the cities along the Himalayan arc and its contiguous regions to estimate the current level of seismic progression.

A key aspect in natural time analysis is the accurate modeling of the interevent counts arising from an ordered pair of earthquake occurrences. The time-dependent nowcasting approach developed on the interevent small earthquake counts also provides an implicit physical interpretation of regional earthquake dynamics characterized by the cycles of recharge (stress buildup) and discharge (stress release) associated with large events (Rundle and Donnellan 2020). The method has been useful in regional or global seismic and tsunami hazard estimation [e.g., 213, 240, 244, 246], induced seismicity analysis [e.g., 156], and in earthquake forecasting through a natural time Weibull projection [e.g., 102, 241]. Nonetheless, the present version of the nowcasting technique does not attribute to the "long-term fault memory" of earthquake "supercycles", nor it describes the fault geometry and kinematic parameters [250, 256].

6.6.1 Validation of EPS in the northwest Himalaya

The nowcast scores, interpreted as a way of assessing tectonic stress build-up at the current time, also yield useful information for strategic planning. However, it is important to keep in mind that in NTA or any statistical data-driven analysis, early failures (much more before than the "expected number of natural time counts") are inevitable phenomena, reflecting the variability in natural time statistics [119, 213]. To clarify, the NTA of two cities in Pakistan, namely Islamabad (the capital city) and Peshawar is considered. The last large earthquakes ($M \geq 6.0$) in Islamabad and Peshawar circular city regions are the October 08, 2005 M_w=7.6 Kashmir earthquake and the most recent December 20, 2019 M_w=6.1 Hindu Kush region earthquake, respectively. Before the 2005 event, the Islamabad city region has also experienced two large-sized events on November 20, 2002 (M_w=6.3) and May 20, 1992 (M_w=6.0) among eight such events since 1972. At the onset

of these earthquakes, the natural time counts of the Islamabad region were 75 and 193, respectively, with the equivalent nowcast scores 54 percent (prior to the 2005 Kashmir earthquake) and 90 percent (prior to the 2002 Astor Valley earthquake). This shows that the disastrous 2005 Kashmir earthquake occurred with just an estimated EPS score of 54 percent. Similarly, for the Peshawar city region that has proximity to the active tectonism of Hindu Kush mountain belt in Pakistan-Afghanistan border, the nowcast scores (%) prior to the latest three large events on December 20, 2019 (M_w=6.1), August 08, 2019 (M_w=6.2) and May 10, 2018 (M_w=6.3) read as 46, 83 and 96, respectively. This implies that the December 2019 major earthquake in the Peshawar city region occurred with just an estimated nowcast value of 46 percent. Besides the consideration of statistical variability in natural time counts, it is re-emphasized that the present nowcasting analysis does not necessarily have any direct implication on the future seismic activity of a region. For example, although the "current" state of earthquake hazard and related seismic risk of the Peshawar city is towards a lower side (EPS = 43%), it may observe a rapid growth in EPS score in a very short span of time due to a much higher background seismicity rate in the adjacent Hindu Kush regions. In contrast to Peshawar, the current state of seismic hazard in the New Delhi region (EPS = 56%) may observe a sluggish growth over time. Apart from a couple of cities (e.g., New Delhi and Peshawar), the current level of seismic progression in the earthquake cycle of large size events is alarmingly high throughout the northwestern part of the Himalayan orogeny.

6.6.2 Validation of EPS in the central Himalaya

To provide a validation of EPS in the central Himalaya, the EPS scores (%) for five metropolitan cities prior to the 2015 M_w 7.8 Gorkha earthquake are as Bharatpur (84), Birganj (79), Kathmandu (87), Lalitpur (86), and Pokhara (73). In addition, as the 2015 M_w 7.8 event did not strike some of the remaining city regions, their EPS scores corresponding to the previous large event are also discussed. Prior to the 1999 M_w 6.6 Chamoli earthquake, the present analysis would assign 81% EPS score for Dhangadhi and 56% for Bhimdatta. Similarly, prior to the 2011 event, the present analysis would assign EPS scores as Biratnagar (86%), Birtamod (86%), Damak (82%), Dharan (84%), Itahari (83%), and Janakpur (86%), and prior to the 2015 event, the present analysis would assign EPS scores for other cities as Budhanilkantha (87%), Butwal (91%), Jitpur Simara (81%), Ghorahi (96%), Gokarneshwar (88%), Hetauda (84%), Kalaiya (80%), Tilotamma (90%), and Tulsipur (97%). The above scores prior to the 1999, 2011 or the

2015 “large” event well demonstrate the validation of the nowcasting method along the central Himalaya.

6.6.3 Validation of EPS in the northeast Himalaya

To provide a validation of EPS in the northeast Himalaya, eight city regions (i.e., Dibrugarh, Dimapur, Gangtok, Guwahati, Itanagar, Kohima, Siliguri, and Sylhet) are considered and their nowcast scores corresponding to two previous seismic cycles are analyzed. The EPS scores (%) turn out to be 94 and 85 (Dibrugarh), 83 and 97 (Dimapur), 33 and 76 (Gangtok), 67 and 74 (Guwahati), 66 and 95 (Itanagar), 87 and 98 (Kohima), 38 and 80 (Siliguri), and 75 and 83 (Sylhet), respectively. Therefore, apart from a few instances of “infant mortality”, the estimated nowcast scores demonstrate their usefulness.

Based on the above discussion, it has been observed that the nowcasting method is one of the prominent methods to determine the current state of regional earthquake hazard in terms of EPS.

6.6.4 Regions of high seismic hazard from the combination of EPS and moment deficits

Seismic hazard assessment using geodetic methods (Chapter 3 to Chapter 5) and using statistical methods (Chapter 6) are all related to the concept of elastic rebound, that is, energy release and accumulation. While the geodetic approach provides a long-term prospective (about $\sim$900 years) of strain accumulation, the proposed nowcasting approach determines the current progression of earthquake cycle in several target localities. It may be recalled that high seismic hazard was observed along various segments (e.g., central seismic gap) using moment deficit rates (Chapter 5). These segments, in general, also exhibit high EPS scores (e.g., central seismic gap in Nepal Himalaya). As a consequence, the combination of these two methods provide a snapshot of high seismic hazard areas along the Himalayan arc.

6.7 Summary

To statistically address the current state of regional earthquake hazard at a dozen populous cities along the Himalayan subcontinent, the present chapter has focused on an empirical data-driven technique, known as earthquake nowcasting. In this method, the natural

times, the cumulative number of intermittent small magnitude events between pairs of large earthquakes, is utilized to mark the evolution of the seismic process rather than the traditional clock or calender times. A number of reference probability distributions are fitted to the observed natural time counts to compute the EPS of 74 circular city regions. The analysis leads to the following remarks:

1. Unlike the seismic hazard assessment through the geodetic measurements (Chapter 3 to Chapter 5), the present chapter utilizes a statistical earthquake nowcasting approach.

2. The EPS for cities along the northwest Himalaya is alarmingly high, except New Delhi (56%) and Peshawar (38%).

3. The EPS for cities along the central Himalaya suggests that almost all cities, except Ghorahi (67%) and Tulsipur (59%), have progressed to their rear end of the seismic cycle. However, the seismic risk remains same for all the cities due to the Poisson nature of seismicity.

4. The EPS for cities along the northeast Himalaya and its adjacent regions varies between 41% to 94%, with the scores (>75%) of Agartala (91), Aizawl (84), Brahmanbaria (90), Chittagong (94), Comilla (88), Darjeeling (81), Dhaka (78), Dimapur (80), Gazipur (79), Imphal (90), Kohima (85), Manikganj (70), Mymensingh (81), Narayanganj (77), and Silchar (87).

5. The EPS results are observed to be generally consistent to the changes of parameter values.

The present chapter has discussed contemporary state of regional earthquake hazard in 74 populous cities of Himalayan subcontinent through the nowcasting technique. The next chapter 7 will summarize the entire thesis work along with a few recommendations.